

# CsMn(Br<sub>x</sub>I<sub>1-x</sub>)<sub>3</sub>: Crossover from an XY to an Ising chiral antiferromagnet

R. Bügel,<sup>1</sup> J. Wosnitza,<sup>1</sup> H. v. Löhneysen,<sup>1</sup> T. Ono,<sup>2</sup> and H. Tanaka<sup>2</sup>  
<sup>1</sup>Physikalisches Institut, Universität Karlsruhe, D-76128 Karlsruhe, Germany  
<sup>2</sup>Department of Physics, Tokyo Institute of Technology, Tokyo 152, Japan  
 (Received 1 March 2001; published 2 August 2001)

We report on high-resolution specific-heat and magnetocaloric-effect measurements of the triangular-lattice antiferromagnets CsMn(Br<sub>x</sub>I<sub>1-x</sub>)<sub>3</sub> with different  $x$ . The evolution of the magnetic phase diagrams from the easy-axis system for  $x=0$  to the easy-plane system for  $x=1$  was studied in detail. The specific-heat critical exponent  $\alpha$  of the almost isotropic  $x=0.19$  system agrees with the value predicted for a chiral Heisenberg scenario. In an applied magnetic field ( $B=6$  T) a crossover to a weak first-order transition is detected.

DOI: 10.1103/PhysRevB.64.094406

PACS number(s): 75.40.Cx, 75.50.Ee

## I. INTRODUCTION

The triangular-lattice antiferromagnets  $ABX_3$  with CsNiCl<sub>3</sub> structure, where the magnetic  $B^{2+}$  ions form a triangular lattice, exhibit frustration due to the antiferromagnetic interactions on a triangular plaquette if the magnetic moments have a component in the triangular  $ab$  plane. The magnetic moments then form a 120° structure, with the extra twofold degeneracy of chirality being broken at the antiferromagnetic transition. Simply speaking, the extra degeneracy arises from the possibility that the 120° spin structure on a given plaquette can be arranged clockwise or counterclockwise when moving around the plaquette. It has been suggested that the chiral degeneracy leads to new universality classes for three-dimensional XY and Heisenberg models.<sup>1,2</sup> The largest changes of the critical exponents are predicted to occur in the specific-heat exponent  $\alpha$ , where the chiral XY and chiral Heisenberg universality classes are predicted to show  $\alpha=0.34$  and  $0.24$ , compared to  $\alpha=-0.01$  and  $-0.12$  for the standard XY and Heisenberg models, respectively.<sup>2</sup> This scenario has been confirmed very recently by a sixth-order field-theoretical expansion.<sup>3</sup> However, whether this concept of new universality classes is indeed applicable is a strongly debated question. Especially within recent years theoretical studies have supplied growing support for a weakly first-order scenario for both chiral phase transitions (see Refs. 4–6 and references therein). An experimental indication for this behavior was found recently.<sup>7</sup>

In any case, the frustration enhances the degeneracy giving rise to different physics with rich phase diagrams and strongly modified critical behavior, which has been studied experimentally for a large number of different triangular-lattice antiferromagnets.<sup>8</sup> A well-studied example is the easy-plane system CsMnBr<sub>3</sub>, for which a number of experiments<sup>9–13</sup> revealed a critical behavior in line with the theoretical prediction.<sup>2</sup> For  $ABX_3$  systems with easy-axis anisotropy like CsMnI<sub>3</sub> (as well as CsNiCl<sub>3</sub>), chiral behavior can be induced by applying a spin-flop field along the easy  $c$  direction thus forcing the spins into the  $ab$  planes. At the spin-flop field  $B_M$  ( $\sim 6.4$  T for CsMnI<sub>3</sub> and  $\sim 2.3$  T for CsNiCl<sub>3</sub>) the magnetic energy is equal to the anisotropy energy, i.e., full isotropy in spin space is attained and chiral Heisenberg behavior is found.<sup>14–17</sup> For higher fields, an easy-

plane anisotropy is induced and XY chirality occurs.<sup>16,17</sup>

Not many triangular-lattice antiferromagnets with negligible anisotropy exist. Besides the above-mentioned materials at their spin-flop fields, only the hexagonal antiferromagnet VBr<sub>2</sub> is known. Indeed, for VBr<sub>2</sub> critical exponents were found in line with the behavior predicted for a chiral Heisenberg system.<sup>18</sup> The possibility to tune a chiral Heisenberg system is offered by the solid solution CsMn(Br<sub>x</sub>I<sub>1-x</sub>)<sub>3</sub> that spans the range from an easy-axis system ( $x=0$ ) to an easy-plane system ( $x=1$ ). This system, therefore, allows us to study the crossover in the magnetic phase diagrams and its influence on the critical behavior. In particular, the composition with  $x=0.19$  presents an almost isotropic system and should therefore follow chiral Heisenberg behavior.<sup>19</sup> Magnetization measurements of CsMn(Br<sub>x</sub>I<sub>1-x</sub>)<sub>3</sub> that gave some information on the magnetic phase diagrams have already been reported by Ono *et al.*<sup>19</sup> Here we report on detailed specific-heat and magnetocaloric-effect measurements.

The spin Hamiltonian that describes the system is given by

$$\mathcal{H} = -J_c \sum_{i,j}^{\text{chain}} \mathbf{S}_i \cdot \mathbf{S}_j - J_{ab} \sum_{i,j}^{\text{plane}} \mathbf{S}_i \cdot \mathbf{S}_j + D \sum_i (S_i^z)^2 - g \mu_B \sum_i \mathbf{B} \cdot \mathbf{S}_i. \quad (1)$$

The summation  $(i,j)$  is over nearest neighbors, with the first sum along the  $c$  direction and the second sum in the  $ab$  plane, with the exchange constants  $J_c$  and  $J_{ab}$ , respectively.  $D < 0$  corresponds to an easy-axis system,  $D > 0$  to an easy-plane system. For CsMnBr<sub>3</sub>,  $J_c = -0.89$  meV,  $J_{ab} = -1.7$   $\mu$ eV, and  $D = 12$   $\mu$ eV,<sup>20</sup> for CsMnI<sub>3</sub>,  $J_c = -1.5$  meV,  $J_{ab} = -7.6$   $\mu$ eV, and  $D = -3.8$   $\mu$ eV.<sup>21</sup> For both materials we are dealing with the  $S=5/2$  spins of Mn<sup>2+</sup>.

The topology of the magnetic phase diagrams for  $ABX_3$  antiferromagnets depends crucially on the sign of  $D$  and on the ratio  $D/J_{ab}$ . Systems with Ising anisotropy ( $D < 0$ ) show two successive phase transitions at  $T_{N1}$  and  $T_{N2}$  for  $B=0$  (see, e.g., Refs. 14, 16, and 17). In the low-temperature phase ( $T < T_{N2}$ ) the spins order in three sublattices where one-third of the spins align along the  $c$  axis, whereas the other two-

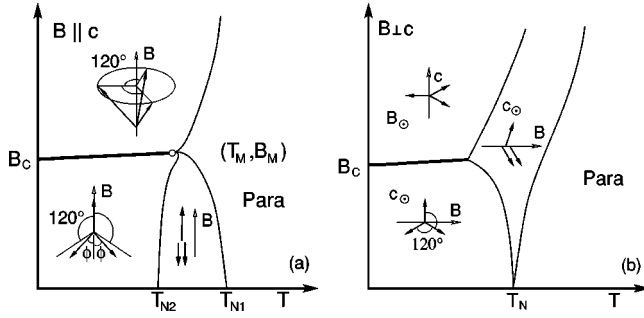


FIG. 1. (a) Schematic phase diagram of a triangular-lattice antiferromagnet with easy-axis anisotropy ( $D < 0$ ) for  $B \parallel c$ . The phase lines meet at the multicritical point  $(T_M, B_M)$ .  $B_c$  is the critical field for the spin-flop transition. (b) The schematic phase diagram for systems with a small easy-plane anisotropy  $0 < D < 3|J_{ab}|$  for  $B \perp c$ . The insets sketch the spin arrangements.

thirds are tilted by an angle  $\Phi$  [which depends on the ratio  $D/J_{ab}$  (Ref. 8)] with respect to the  $c$  axis [see Fig. 1(a)]. For  $\text{CsMnI}_3$  this angle is  $\Phi = 51^\circ$ .<sup>21</sup> All spins lie within a plane that includes the  $c$  axis. At higher temperatures in the intermediate phase ( $T_{N2} < T < T_{N1}$ ) the tilted spins have an additional degree of freedom, i.e., their components within the basal  $ab$  plane are not defined. For  $T > T_{N1}$  in the paramagnetic phase only short-range ordered independent spin chains exist along the  $c$  axis. For a magnetic field applied within the basal plane ( $B \perp c$ ) the two phase boundaries shift somewhat to higher temperatures (at least up to 6 T for  $\text{CsMnI}_3$  and  $\text{CsNiCl}_3$ ) without changing the principal spin topology.<sup>14,22</sup>

Of much more relevance is the case when  $B$  is applied along  $c$  [Fig. 1(a)]. For  $T < T_{N2}$ , a first-order phase transition occurs at the spin-flop field  $B_c$  above which the three sublattices form a  $120^\circ$  umbrellalike structure. The  $c$ -axis spin component grows with further increasing  $B$ . For classical spins with  $J_c \gg J_{ab}$ ,  $B_c$  at  $T=0$  is given by

$$(g\mu_B B_c)^2 = 16|J_c D|S^2. \quad (2)$$

At the multicritical point  $(T_M, B_M)$  the three phase lines merge tangentially into the first-order spin-flop line.<sup>23,24</sup> At this point full isotropy in spin space is achieved that leads to a chiral Heisenberg universality as experimentally observed for  $\text{CsNiCl}_3$  (Refs. 16 and 17) and  $\text{CsMnI}_3$ .<sup>14</sup>

For systems with easy-plane anisotropy ( $D > 0$ ) only one phase transition at  $T_N$  from the paramagnetic to the chiral  $120^\circ$  structure exists at  $B=0$ . The critical behavior, therefore, is of the chiral  $XY$  type. A magnetic field applied along the  $c$  direction does not change the symmetry of the ground state. Consequently, the critical behavior stays essentially constant.<sup>12</sup> A much richer phase diagram can be observed for  $B \perp c$ . The phase diagram as predicted for  $D < 3|J_{ab}|$  is shown in Fig. 1(b).<sup>25</sup> At  $T < T_N$  and  $B < B_c$  the chiral phase exists. The competition between the Zeeman energy and the anisotropy energy leads to a spin-flop phase above  $B_c$  that is also given by Eq. (2).<sup>8</sup> Thereby, the spin triangle is oriented perpendicularly to  $B$ . Between the chiral low-temperature and the paramagnetic high-temperature phase, a collinear spin structure evolves where the spins remain in the  $ab$  plane

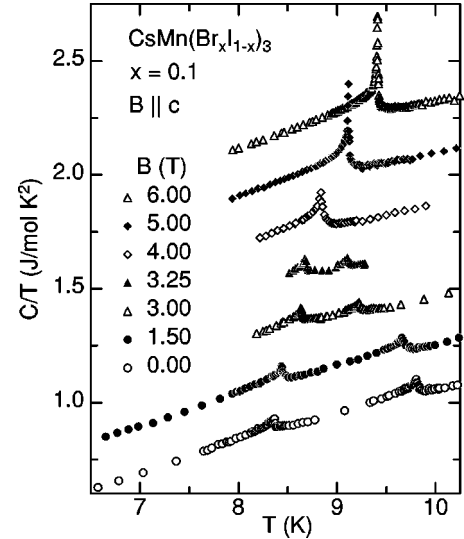


FIG. 2. Specific heat  $C$  divided by temperature  $T$  vs  $T$  for  $\text{CsMn}(\text{Br}_{0.1}\text{I}_{0.9})_3$  in a magnetic field  $B$  parallel to the  $c$  direction. Data are shifted consecutively by  $0.2 \text{ J/mol K}^2$  with respect to  $B=0$ .

with two spins of a triangle pointing parallel and one in the opposite direction. With increasing field the spin components along  $B$  become larger.

Experimentally, very little is known about the phase diagrams and the critical properties of easy-plane systems with such a small anisotropy ( $D < 3|J_{ab}|$ ).<sup>8</sup> On the other hand, for materials with  $D > 3|J_{ab}|$ , like  $\text{CsMnBr}_3$ , the phase diagram has been very well established.<sup>10,14,26</sup> Due to the stronger anisotropy  $D$  the spin-flop phase is absent for such  $XY$  systems with only the chiral phase and the collinear structure remaining.<sup>8</sup>

## II. EXPERIMENT

Single-crystalline samples of  $\text{CsMn}(\text{Br}_x\text{I}_{1-x})_3$  were grown by the Bridgman technique at the Tokyo Institute of Technology.<sup>19</sup> For the measurements pieces of 24–111 mg were cleaved from the crystals. The specific heat  $C$  was measured by a standard semiadiabatic heat-pulse technique. Magnetic fields up to 14 T were applied either along or perpendicular to the clearly visible  $c$  axis of the crystals. The magnetocaloric effect,  $(\delta T/\delta B)_S = -(T/C)(\delta S/\delta B)_T$ , was measured in the same calorimeter.  $S$  denotes the entropy of the system. Upon changing the magnetic field by small steps  $\Delta B$ , the resulting temperature variation  $\Delta T$  was recorded. Taking into account the small eddy-current heating the magnetocaloric effect  $\Delta T/\Delta B$  was extracted. For more details on the experiment see Ref. 27.

## III. RESULTS AND DISCUSSION

The specific heat of the sample with the smallest Br concentration,  $\text{CsMn}(\text{Br}_{0.1}\text{I}_{0.9})_3$ , is shown in Fig. 2 for different fields  $B$  aligned along the  $c$  direction. This easy-axis system shows two consecutive zero-field transitions, which merge into one at the spin-flop field of about 4 T. The steep

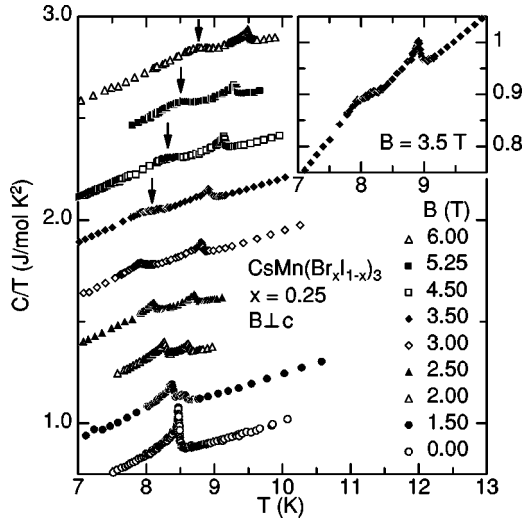


FIG. 3.  $C/T$  vs  $T$  for  $\text{CsMn}(\text{Br}_{0.25}\text{I}_{0.75})_3$  in  $B \perp c$ . Data are shifted consecutively by  $0.2 \text{ J/mol K}^2$  with respect to  $B=0$ . The arrows indicate the phase transitions between the spin-flop phase and the intermediate collinear phase. The inset shows an enlargement of the data at  $B=3.5 \text{ T}$ .

anomaly found beyond this field resembles that found for pure  $\text{CsMnI}_3$  that was analyzed in terms of a chiral Heisenberg model at the spin-flop field  $B_M \approx 6.4 \text{ T}$ .<sup>14</sup> The substitution of 10% of the  $\text{I}^-$  ions by  $\text{Br}^-$  with the concomitant increase of the (negative) anisotropy  $D$  towards zero reduces considerably the spin-flop field and likewise the width of the intermediate phase ( $T_{N2}=8.36 \text{ K} < T < T_{N1}=9.80 \text{ K}$ ). This trend continues further for a sample with  $x=0.18$  (data not shown) where  $T_{N1}=8.50 \text{ K}$ ,  $T_{N2}=8.40 \text{ K}$ , and  $B_M \approx 1 \text{ T}$  (see also Figs. 6 and 7 below).

The data for  $x=0.25$ , on the other hand, resemble those of the pure easy-plane system  $\text{CsMnBr}_3$ ,<sup>14,26</sup> where a magnetic field in the  $ab$  plane quickly removes the chiral degeneracy and leads to a splitting of the zero-field transition (Fig. 3). In contrast to pure  $\text{CsMnBr}_3$ , however, the anomaly at lower temperatures changes its appearance above about 3 T, i.e., the anomaly (visualized by the arrows in Fig. 3) becomes much more rounded and the feature in  $C$  shifts towards higher temperatures for increasing  $B$  rather than to lower  $T$  as in  $\text{CsMnBr}_3$ .<sup>14,26</sup> Indeed, what is reflected by the low-temperature anomalies in Fig. 3 are two different phase transitions; from the chiral phase to the collinear phase at low  $B$  and from the spin-flop phase to the collinear phase at  $B$  larger than about 3 T [see Fig. 1(b) and also the phase diagram in Fig. 6 below]. This result, therefore, reflects the fact that the anisotropy  $D$  for  $x=0.25$  has switched from negative to positive, with  $D < 3|J_{ab}|$ . We found a similar behavior with a considerably reduced width of the collinear phase in the specific heat of a sample with  $x=0.20$  (data not shown).

Consequently, the anisotropy  $D$  should become zero somewhere between  $x=0.18$  and  $x=0.20$ . A good candidate for such a chiral Heisenberg system is therefore  $\text{CsMn}(\text{Br}_{0.19}\text{I}_{0.81})_3$ . For an isotropic Heisenberg system only one phase-transition line from the paramagnetic to the chiral phase is expected, independent of the magnetic-field orientation. Indeed, magnetization and susceptibility data could not

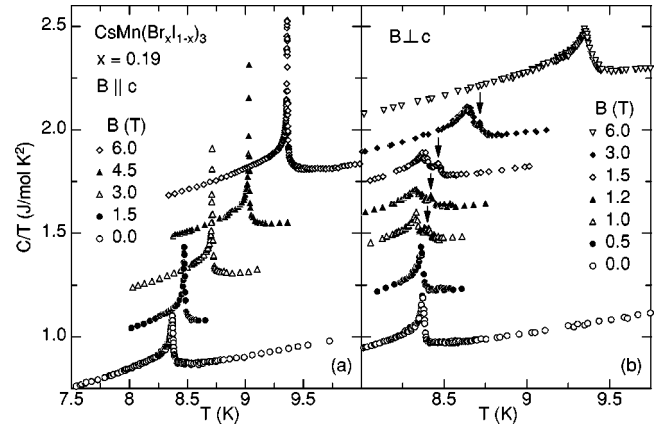


FIG. 4.  $C/T$  vs  $T$  for  $\text{CsMn}(\text{Br}_{0.19}\text{I}_{0.81})_3$  in magnetic fields (a)  $B$  parallel and (b)  $B$  perpendicular to the  $c$  direction. Data are shifted by different amounts with respect to  $B=0$ . The arrows highlight the small anomaly indicating the transition from the intermediate phase to the paramagnetic phase.

observe any spin-flop line or splitting of the zero-field transition.<sup>19</sup> Our specific-heat data for  $B \parallel c$  [Fig. 4(a)] are in line with these observations. We particularly can resolve only a single strong anomaly at  $T_N$  that becomes somewhat larger with increasing field up to 6 T, similar to what is observed for  $x=0.1$  above  $B_M$ .

However, measurements of  $\text{CsMn}(\text{Br}_{0.19}\text{I}_{0.81})_3$  for  $B \perp c$  [Fig. 4(b)] reflect a small residual planar anisotropy, as evidenced by a slight splitting of the transition in fields between 1 and 3 T. The anomaly at lower temperatures is still relatively sharp and large at  $B=1 \text{ T}$ , but becomes clearly reduced at 1.2 T that indicates the junction with the spin-flop phase line. At higher fields the phase lines merge and only one anomaly remains at 6 T.

In order to determine the complete phase diagrams including the expected spin-flop lines (see Fig. 1) we measured the magnetocaloric effect for all samples. Since the spin-flop transition at  $B_c$  is almost temperature independent, the specific heat is not sensitive to this transition, contrary to magnetocaloric-effect measurements that cross the corresponding phase line at an approximately right angle. Figure 5(a) shows the magnetocaloric effect for the samples with  $x=0.18$  and  $x=0.19$  at  $T \approx 7 \text{ K}$  in fields aligned parallel to the  $c$  axis. For  $x=0.18$ , a clear step at about 0.9 T is visible that signals the spin-flop transition in line with the data of Ono *et al.*<sup>19</sup> The spin-flop field at each temperature was estimated from the position of the maximum in the derivative of the magnetocaloric-effect data. For  $x=0.19$ ,  $\Delta T/\Delta B$  increases monotonically without any detectable step or anomaly. This confirms that  $\text{CsMn}(\text{Br}_{0.19}\text{I}_{0.81})_3$  has no Ising-like anisotropy.

Instead the anisotropy  $D$  has switched to an XY type, as the specific-heat data [Fig. 4(b)] show. Consequently, a spin-flop line is expected for fields perpendicular to  $c$  [see Fig. 1(b)]. Indeed, magnetocaloric-effect data could verify this phase diagram by showing a steplike feature at about 1.2 T almost independent of temperature [Fig. 5(b)]. Therefore, the critical concentration for which  $D=0$  should be just below  $x=0.19$ .

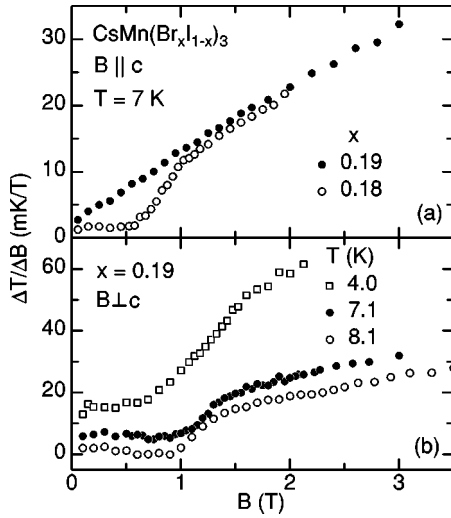


FIG. 5. Magnetocaloric effect of (a)  $\text{CsMn}(\text{Br}_x\text{I}_{1-x})_3$  and  $\text{CsMn}(\text{Br}_{0.18}\text{I}_{0.82})_3$  in  $B \parallel c$  and (b) of  $\text{CsMn}(\text{Br}_{0.19}\text{I}_{0.81})_3$  for three different temperatures in  $B \perp c$ . Data in (b) are shifted consecutively by 5 mK/T with respect to  $T = 8.1$  K.

Figure 6 summarizes the results in terms of  $(B, T)$  phase diagrams for various  $x$ . In Fig. 6(a), the absolute magnitude of the easy-axis anisotropy ( $D < 0$ ) decreases with increasing  $x$ , getting close to zero for  $x = 0.18$ . From the reduced spin-flop field  $B_c \approx 1$  T for  $x = 0.18$  one can estimate with Eq. (2) that  $|J_c D|$  has reduced to about 2.5% of the value for  $\text{CsMnI}_3$ . Since  $J_c$  should depend little on  $x$ , this means that  $|D|$  has reduced to about 95 neV corresponding to 1.1 mK. The phase diagrams for  $x = 0.10$  and  $x = 0.18$  fully agree with the predicted behavior for easy-axis systems [Fig. 1(a)].<sup>8</sup>

The phase-diagram topology changes for easy-plane systems with  $D > 0$ . In Fig. 6(b), the absolute magnitude of  $D$  increases with  $x$ , with a small anisotropy present for  $x = 0.19$ . As for  $B \parallel c$ , the phase diagrams for  $B \perp c$  ( $D > 0$ ) are in full agreement with mean-field calculations and verify

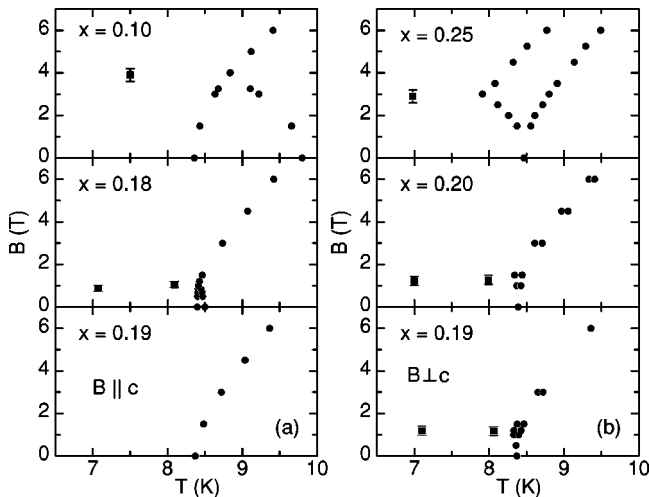


FIG. 6. Phase diagrams of  $\text{CsMn}(\text{Br}_x\text{I}_{1-x})_3$  (a) for fields along the  $c$  direction for  $x \leq 0.19$  and (b) for fields perpendicular to  $c$  for  $x \geq 0.19$ .

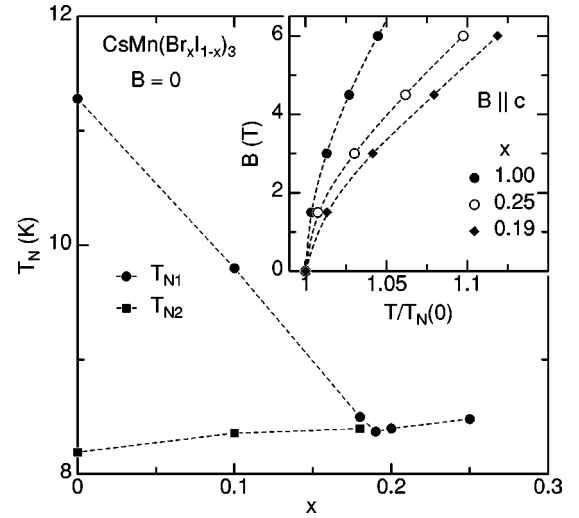


FIG. 7. Transition temperatures  $T_{N1}$  and  $T_{N2}$  of  $\text{CsMn}(\text{Br}_x\text{I}_{1-x})_3$  at  $B = 0$  as a function of  $x$ . The data for  $\text{CsMnI}_3$  are from Ref. 22. Lines are guide to the eye. The inset shows the field dependence of the normalized transition temperatures for three concentrations in  $B \parallel c$ .

nicely the predictions for easy-plane systems with  $D < 3|J_{ab}|$ .<sup>25</sup>

The phase diagram of the transition temperatures vs Br concentration  $x$  is shown in Fig. 7. The lower Néel temperature  $T_{N2}$  increases slightly with  $x$ , whereas  $T_{N1}$  rapidly decreases. The two phase lines merge at a critical concentration  $x_c$  somewhere between  $x = 0.18$  and  $x = 0.19$ . The phase diagram is in line with that reported by Ono *et al.*<sup>19</sup> With our specific-heat and magnetocaloric-effect measurements, however, we were able to resolve the spin-flop line and the intermediate collinear phase for  $x = 0.19$  at fields between 1 and 3 T proving that the critical concentration with  $D = 0$  must be slightly less than  $x = 0.19$ .

For completeness, the inset of Fig. 7 shows a comparative  $B$ - $T$  phase diagram for different chiral  $XY$  systems with  $B$  aligned along the  $c$  direction. The data for  $\text{CsMnBr}_3$  are from Ref. 28. With increasing field the phase transition from the paramagnetic to the chiral phase shifts to higher temperatures. This effect is less prominent for larger  $x$  indicating that the field-induced  $T_N$  increase becomes larger for reduced  $D$ .

As a final point, we discuss the critical behavior of  $\text{CsMn}(\text{Br}_x\text{I}_{1-x})_3$ . In order to describe the specific-heat data close to the critical temperature  $T_c$  we applied the usual fit function<sup>29</sup>

$$C^\pm = (A^\pm/\alpha)|t|^{-\alpha} + B + Et, \quad (3)$$

where  $t = (T - T_c)/T_c$  and the superscript  $+$  ( $-$ ) refers to  $t > 0$  ( $t < 0$ ). The first term describes the leading contribution to the singularity in  $C$  and the nonsingular contribution to the specific heat is approximated by  $B + Et$ . After a good fit of the data had been achieved except very close to  $T_c$ , a Gaussian distribution of  $T_c$  with width  $\delta T_c$  was introduced. This procedure is able to describe a rounding of the transitions caused by sample inhomogeneities (see also Refs. 14 and 15).

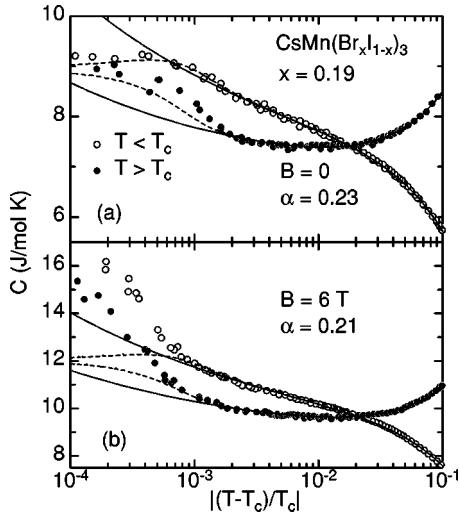


FIG. 8. Specific heat  $C$  of CsMn(Br<sub>0.19</sub>I<sub>0.81</sub>)<sub>3</sub> vs  $\ln|(T-T_c)/T_c|$  for (a)  $B=0$  and (b)  $B=6$  T. The solid lines are fits according to Eq. (3), the dash-dotted lines are fits including a Gauss-distributed smearing of  $T_c$ .

Figure 8(a) shows the specific heat  $C$  for  $x=0.19$  vs the reduced temperature  $|t|$  at  $B=0$ . The data are compatible with an exponent  $\alpha=0.23(7)$  of the specific heat if we include a Gaussian broadening of  $\delta T_c/T_c \approx 4.2 \times 10^{-4}$ . The dashed lines indicate the fit with these parameters, while the solid lines represent a fit with  $\delta T_c=0$ . The exponent  $\alpha$  as well as the experimental amplitude ratio  $A^+/A^- = 0.54(13)$  are in line with the chiral Heisenberg model, which predicts  $\alpha=0.24(8)$  and  $A^+/A^- = 0.54(20)$ .<sup>2</sup> This is in accordance with the small easy-plane anisotropy that obviously is too small to force the system to XY chirality. The available results of neutron-scattering experiments for  $x=0.19$  are rather inconclusive.<sup>30</sup> While the exponent  $\beta=0.28(2)$  of the sublattice magnetization agrees well with the theoretical value of a chiral Heisenberg system ( $\beta=0.30$ ), the exponents of the susceptibility,  $\gamma=0.75(4)$ , and of the correlation length,  $\nu=0.42(3)$ , are at variance with the predictions ( $\gamma=1.17$  and  $\nu=0.59$ ). Furthermore, the experimentally found exponents are in contradiction with the fundamental scaling laws  $\alpha+2\beta+\gamma=2$  and  $\alpha+d\nu=2$  ( $d$  is the dimension), which should be fulfilled at universal second-order phase transitions.

Theoretically, the region around the multicritical point where a chiral Heisenberg scenario is expected should not be large.<sup>31</sup> This would imply that either the increase of the Br concentration ( $x > x_c$ ) or the application of a large magnetic field ( $B > B_M$ ) should drive the system quickly to chiral XY

behavior with  $\alpha=0.34(6)$ , which for CsMnBr<sub>3</sub> ( $x=1$ ) has been observed.<sup>11,12</sup> Nevertheless, for  $x=0.20$  and for  $x=0.25$  the critical exponents remain approximately constant with  $\alpha=0.25(7)$  and  $\alpha=0.20(6)$ , respectively, suggesting that the chiral Heisenberg behavior is rather stable.

Another unexpected result becomes obvious from the analysis of the specific-heat data of  $x=0.19$  in  $B=6$  T applied along the  $c$  direction [Fig. 8(b)]. A magnetic field of this strength, i.e., much larger than  $B_M$ , should induce XY chirality for a system with Ising anisotropy as previously observed for CsNiCl<sub>3</sub> (Refs. 16 and 17) and, in this work, with  $\alpha=0.37(10)$  for CsMn(Br<sub>0.1</sub>I<sub>0.9</sub>)<sub>3</sub> at  $B=6$  T (not shown). Likewise, for an easy-plane system like CsMnBr<sub>3</sub> the critical behavior remains chiral XY-like for fields applied along  $c$ .<sup>12</sup> However, for  $x=0.19$  (as well as for  $x=0.18$ , data not shown) in a magnetic field of 6 T,  $C$  for  $t \geq 10^{-3}$  still follows a chiral Heisenberg-like behavior with  $\alpha=0.21(8)$  [ $\alpha=0.23(6)$  for  $x=0.18$ ] and increases much more strongly for  $t \rightarrow 0$ , which can neither be described by a reasonable critical exponent nor by a  $T_c$  distribution. This possibly indicates a crossover to a weakly first-order transition, similar as previously observed for CsCuCl<sub>3</sub> close to  $T_c$  at  $B=0$ .<sup>7</sup>

In conclusion, we have mapped out in detail the impact of an axial vs a planar anisotropy on the magnetic phase diagrams of triangular-lattice antiferromagnets by fine tuning  $x$  of the system CsMn(Br <sub>$x$</sub> I <sub>$1-x$</sub> )<sub>3</sub>. In particular, the predicted phase diagram [Fig. 1(b)] of easy-plane systems with small anisotropy could be accurately verified. The critical concentration, for which the spin anisotropy vanishes, was found to be located between  $x=0.18$ , a system with small axial anisotropy ( $D < 0$ ), and  $x=0.19$ , a system with small planar anisotropy ( $D > 0$ ). The critical behavior at  $B=0$  for  $x=0.19$ ,  $x=0.20$ , and  $x=0.25$  can be described with critical exponents  $\alpha$  as predicted from Monte Carlo simulations for the chiral Heisenberg universality class.<sup>2</sup> Thereby, rounding effects due to sample inhomogeneities prevent the possible detection of a crossover to a first-order scenario as proposed recently.<sup>5</sup> In a magnetic field  $B=6$  T, the samples with  $x=0.18$  and  $x=0.19$  show a weakly first-order phase transition. For  $10^{-3} < t < 0.1$ , the data can be described by chiral Heisenberg critical exponents. For all other samples with either larger planar or larger axial symmetry, no indication for a first-order phase transition was detected.

## ACKNOWLEDGMENTS

We acknowledge numerous discussions and insightful comments on various aspects of low-dimensional magnetism by Professor Erwin Müller-Hartmann.

<sup>1</sup>H. Kawamura, J. Phys. Soc. Jpn. **54**, 3220 (1985); **55**, 2095 (1986).

<sup>2</sup>H. Kawamura, J. Phys.: Condens. Matter **10**, 4707 (1998), and references therein.

<sup>3</sup>A. Pelissetto, P. Rossi, and E. Vicari, Phys. Rev. B **63**, R140414 (2001).

<sup>4</sup>D. Loison and K.D. Schotte, Eur. Phys. J. B **5**, 735 (1998).

<sup>5</sup>M. Tissier, B. Delamotte, and D. Mouhanna, Phys. Rev. Lett. **84**, 5208 (2000).

<sup>6</sup>D. Loison and K.D. Schotte, Eur. Phys. J. B **14**, 125 (2000).

<sup>7</sup>H.B. Weber, T. Werner, J. Wosnitzer, H.v. Löhneysen, and U. Schotte, Phys. Rev. B **54**, 15 924 (1996).

- <sup>8</sup>M.F. Collins and O.A. Petrenko, *Can. J. Phys.* **75**, 605 (1997).
- <sup>9</sup>H. Kadowaki, S.M. Shapiro, T. Inami, and Y. Ajiro, *J. Phys. Soc. Jpn.* **57**, 2640 (1988).
- <sup>10</sup>T.E. Mason, B.D. Gaulin, and M.F. Collins, *Phys. Rev. B* **39**, 586 (1989).
- <sup>11</sup>J. Wang, D.P. Belanger, and B.D. Gaulin, *Phys. Rev. B* **66**, 3195 (1991).
- <sup>12</sup>R. Deutschmann, H.v. Löhneysen, J. Wosnitza, R.K. Kremer, and D. Visser, *Europhys. Lett.* **17**, 637 (1992).
- <sup>13</sup>V.P. Plakhty, J. Kulda, D. Visser, E.V. Moskvina, and J. Wosnitza, *Phys. Rev. Lett.* **85**, 3942 (2000).
- <sup>14</sup>H. Weber, D. Beckmann, J. Wosnitza, H.v. Löhneysen, and D. Visser, *Int. J. Mod. Phys. B* **12**, 1387 (1995).
- <sup>15</sup>H.v. Löhneysen, D. Beckmann, J. Wosnitza, and D. Visser, *J. Magn. Magn. Mater.* **140-144**, 1469 (1995).
- <sup>16</sup>D. Beckmann, J. Wosnitza, H.v. Löhneysen, and D. Visser, *Phys. Rev. Lett.* **71**, 2829 (1993).
- <sup>17</sup>M. Enderle, G. Furtuna, and M. Steiner, *J. Phys.: Condens. Matter* **6**, L385 (1994).
- <sup>18</sup>J. Wosnitza, R. Deutschmann, H.v. Löhneysen, and R.K. Kremer, *J. Phys.: Condens. Matter* **6**, 8045 (1994).
- <sup>19</sup>T. Ono, H. Tanaka, T. Kato, and K. Iio, *J. Phys.: Condens. Matter* **10**, 7209 (1998).
- <sup>20</sup>U. Falk, A. Furrer, H.U. Güdel, and J.K. Kjems, *Phys. Rev. B* **35**, 4888 (1987).
- <sup>21</sup>A. Harrison, M.F. Collins, J. Abu-Dayyah, and C.V. Stager, *Phys. Rev. B* **43**, 679 (1991).
- <sup>22</sup>D. Beckmann, J. Wosnitza, H.v. Löhneysen, and D. Visser, *J. Phys.: Condens. Matter* **5**, 6289 (1993).
- <sup>23</sup>M.L. Plumer, K. Hood, and A. Caillé, *Phys. Rev. Lett.* **60**, 45 (1988).
- <sup>24</sup>H. Kawamura, A. Caillé, and M.L. Plumer, *Phys. Rev. B* **41**, 4416 (1990).
- <sup>25</sup>M.L. Plumer, A. Caillé, and K. Hood, *Phys. Rev. B* **39**, 4489 (1989).
- <sup>26</sup>B.D. Gaulin, T.E. Mason, M.F. Collins, and J.Z. Larese, *Phys. Rev. Lett.* **62**, 1380 (1989).
- <sup>27</sup>F. Pérez, T. Werner, J. Wosnitza, H.v. Löhneysen, and H. Tanaka, *Phys. Rev. B* **58**, 9316 (1998).
- <sup>28</sup>R. Deutschmann, J. Wosnitza, and H. v. Löhneysen (unpublished).
- <sup>29</sup>A. Kornblit and G. Ahlers, *Phys. Rev. B* **8**, 5163 (1973).
- <sup>30</sup>T. Ono, H. Tanaka, T. Kato, K. Iio, K. Nakajima, and K. Kakurai, *J. Magn. Magn. Mater.* **177-181**, 735 (1998); T. Ono, H. Tanaka, T. Kato, K. Nakajima, and K. Kakurai, *J. Phys.: Condens. Matter* **11**, 4427 (1999).
- <sup>31</sup>H. Kawamura, *Phys. Rev. B* **47**, 3415 (1993).